Vol. 12(2), pp. 70-83, April-June 2020
DOI: 10.5897/JHF2020.0631
Article Number: F65C57E64057
ISSN: 2006-9782

http://www.academicjournals.org/JHF

ACADEMIC JOURNALS
expand your knowledge

Journal of Horticulture and Forestry

Full Length Research Paper

An analytical assessment of forest cover changes over the last 30 Years in the semi-deciduous forest zone of Togo

Fifonsi Ayélé DANGBO[1]*, Oliver GARDI[2], Kossi ADJONOU[1], Atsu K. Dogbeda HLOVOR[1], Juergen BLASER[2] and Kouami KOKOU[1]

[1]Forest Research Laboratory, Faculty of Sciences, University of Lome, Togo.
[2]School of Agricultural, Forest and Food Sciences, Bern University of Applied Sciences, Länggasse 85, 3052 Zollikofen, Switzerland.

Received 7 April 2020; Accepted 14 May 2020

Understanding dynamics of forest cover is important to monitor change in forest area. The objective of the present study is to develop an approach for assessing forest cover changes in landscapes with high spatial complexity and temporal variation that can allow the generation of robust monitoring information. The forest-cover change maps were produced using time-series of Landsat images, high resolution images from Google Earth, free software R and QGIS. A complete map of forest cover change at 30 m spatial resolution was produced over 603'972 ha. The result was validated by photo-interpretation of 5000 randomly sampled points and on the basis of high-resolution images available in Google Earth (Quickbird) for the year 2018 and Landsat satellite images for the year 2018, 1991 and 2003. The estimated overall accuracy of the forest cover change map is 88.7%. In the study area, the forest area was estimated at 246'915 ha in 1991, 232'741 ha in 2003 and 230'390 ha in 2018. The gross forest loss has increased from 182.5 ha/year in the first period 1991-2003 to 187.47 ha/year in the second period 2003-2018. The corresponding net annual forest loss (incl. regeneration) rates are 0.5% in the first period and 0.1% in the second period. The decrease of the net annual forest loss rate in the second period is attributed to an increase in forest regeneration. This study can be considered as a reproducible approach to map forest-cover change and can support policy approaches towards reducing emissions from deforestation and degradation (REDD+).

Key words: Forest loss, forest gain, multi-date, Landsat, random forest, Togo.

INTRODUCTION

Changes in forest cover affect important ecosystem services, including biodiversity, climate regulation and carbon storage (Achard et al., 2002; Foley et al., 2005). Forest cover change in the tropics is recognized by the international climate change community to be a major contributor to anthropogenic GHG emissions. Most of the net flux of carbon into the atmosphere due to land-cover changes is attributable to deforestation in the tropics, with

*Corresponding author. E-mail: fifonsidangbo@gmail.com. Tel: 0022890997423.

a smaller fraction attributable to forest degradation (Houghton, 2012). As a consequence, a mechanism for Reducing Emissions from Deforestation and Forest Degradation and the role of conservation, sustainable management of forests and enhancement of forest carbon stocks in developing countries (REDD+) has been developed under the United Nations Framework Convention on Climate Change (UNFCCC). REDD+ aims at rewarding developing nations for slowing down deforestation and forest degradation, which is considered a cost effective way to mitigate anthropogenic greenhouse gas emissions, through a compensation mechanism (UNFCCC, 2010). Mapping forest cover change is a key issue for REDD+ program. Despite well established guidelines provided by the international scientific community (GFOI, 2016); Houghton et al. (2010) showed that “REDD+ program, often lack the institutional investment and scientific capacity to begin implementation of a program that can make use of the global observational record”. In order to get access to REDD+ result-based payments, countries require a national forest monitoring system for measuring forest cover and carbon stock changes in forests in an accurate and consistent way, and comparing them to a counterfactual reference level based on historic forest cover changes (UNFCCC, 2015).

In Togo, several factors contribute to the reduction of forest cover. Main drivers of forest degradation and deforestation are traditional slash and burn agriculture, pasture extension, charcoal production, illegal logging and mining activities, with adverse consequences for local climate, soil degradation, livelihoods, biodiversity conservation and GHG emissions (MERF, 2013). The forests of Togo's sub-humid mountainous area constitute the domain of the semi-deciduous dense forests (Ern, 1979), which are now very degraded and disappearing. Several previous studies (Adjonou et al., 2009; Adjossou, 2004; Adjossou and Kokou, 2004) have shown that forests in the sub-humid mountainous area are very fragmented and have practically been reduced to hard-to-reach areas and along rivers. This fact highlights a research question: (1) what forest cover changes can be observed in the study area over the last decades?

Togo, as many tropical countries, has recently joined the REDD+ mechanism with the ambition of creating a new incentive system to reduce forest loss and to restore the integrity of degraded forests (MERF, 2013). In 2012, the global deforestation map produced by the University of Maryland (Hansen et al., 2013) attracted great attention from scientists. However, (Tropek et al., 2014) have shown that this map overestimates forest cover and underestimates the rate of deforestation at local level. Monitoring the evolution of forest cover by remote sensing in forests of Togo's sub-humid mountainous area is a challenge because of the effect of the relief, gradual changes of degradation and regeneration, different forest types that mix up with fallows and secondary forests growing on agricultural land, high temporal dynamic of clearing and regrowth and relatively low net changes of forest cover. This fact highlights the second research question: How can forest cover changes be mapped consistently, in areas with high diversity of forest types, high forest dynamics and low rates of net change?

In the context of REDD+ in Togo, previous work on forest cover mapping has provided valuable insight into vegetation status and different maps were produced. Indeed, German cooperation financed the production of the land use map using RapidEye satellite images in the context of the national inventory in 2014. This mapping exercise was based on automated segmentation and of RapidEye images acquired in 2013/2014 and visual classification of the resulting segments. Then in 2016, the World Bank funded the interpretation of aerial photos taken between 1976 and 1985 using the same methodological approach. To what extent the resulting figures are comparable with the RapidEye map is uncertain and difficult to validate as the aerial images were not co-registered with the RapidEye images. Despite the production of forest cover maps for different dates, further improvements in classification methods for forest cover change are necessary in order to provide accurate and consistent estimates of forest cover change at national and subnational levels. The general objective of the present study is to develop an approach for assessing forest cover changes in landscapes with high spatial complexity and temporal variation, that can consistently be applied for repeated assessments and thus allows the generation of robust monitoring information as for example required for the reporting of changes in forest carbon stocks in the framework of REDD+. The specific objectives are to map and to quantify forest cover changes in different forest landscapes of semi-deciduous forest zone of Togo for the periods 1991-2003 and 2003-2018.

MATERIALS AND METHODS

Study area

The study area corresponds to Togo’s forest’s zone “ecological zone IV” and is located in the southern part of the Atakora Mountains, south-west of Togo, on the border between Togo and Ghana in the region called Togo Mountains or Togo highlands. The study area extends between the latitudes 6° 15 and 8° 20 N and the longitudes 0° 30 and 1° E, and covers an area of 603’972 hectares (Figure 1). The climate prevailing in this area is a Guinean mountain climate characterized by a long rainy season (8-10 months). The mean annual temperatures range from 21 to 25°C and the total annual rainfall ranges vary from 1400 to 1700 mm. This zone contributes significantly to species richness in Togo (Adjossou, 2009). It is the current domain of semi-deciduous forests. The study area shows a strong topographic heterogeneity. The average altitude is 800 m, with peaks at Djogadjeto (972 m) and Liva (950 m). It has a successions of plateaus (plateau of Kloto, Kouma, Danyi, Akposso, Akebou and Adele), where hills along with their

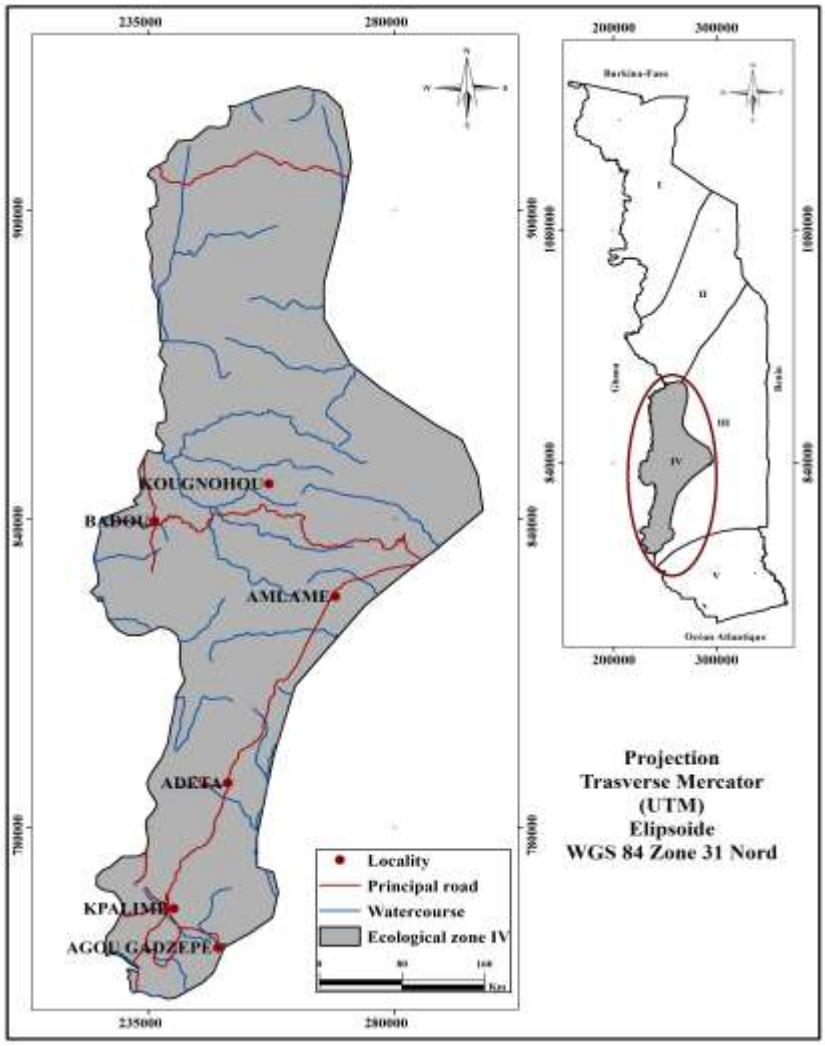

Figure 1. Study area Ecological zone IV.

valleys and caves are common. Landforms are diverse and complex. The main geologic component is of the late Precambrian: Togo and Buem quartzites phyllites, shales and sandstones were largely folded and metamorphosed during the Cambrian Pan-African Orogeny (Hall and Swaine, 1976). A network of complex secondary rivers covers the area with three catchment areas: the basin of the lake Volta in the west of the Mounts and basins of the Mono River and Zio River in the east of the Mounts. Population distribution and land management varies across the area with implications for forest cover changes (Figure 1). The research methodology was based on the following steps:

(i) Acquisition, pre-processing, and stacking of Landsat images.
(ii) Collecting a representative set of training plots for different crown cover densities observed in the region.
(iii) Forest/non-forest classification of reference maps based on training plots using RandomForest.
(iv) Forest/non-forest classification of Landsat time series based on reference maps, again using RandomForest.
(v) Cleaning of time-series using majority filters.
(vi) Accuracy assessment of resulting maps using a set of independent validation plots. These steps are outlined in Figure 3.

Landsat image collection and pre-processing

Landsat-type data has been proven useful for national-scale land cover and land cover change assessments for minimal mapping units (MMU's) of about 1 ha (Achard et al., 2014). A number of other national or regional forest cover change maps have been produced based on the analysis of full coverage of Landsat data (Achard et al., 2014; Grinand et al., 2013; Hansen et al., 2013). The study area is covered by two WRS2 scenes with path 193 and rows 054 and 055. Landsat surface reflectance data at the end of the dry period (Jan - Feb) with less than 10% cloud cover were downloaded from the U.S. Geological Survey (USGS) Center for Earth Resources Observation and Science (EROS) portal (https://earthexplorer.usgs.gov/) at full spatial and spectral resolution (30 x 30 m resolution). The data selected was for the end of dry season as forests can then be best distinguished from other types of vegetation and classification tends to be more accurate than during the wet season (Liu et al., 2015). Furthermore, the availability of cloud-free images is limited in wet season in comparison to dry season.

The final dataset obtained consists of a series of 15 geometrically and radiometrically corrected images from the satellites Landsat

Figure 2. Examples of visual interpretation of training plots (30x30m) for crown cover using QGIS and QuickBird/GoogleEarth images 2018. 1/9 means that 1 of the 9 cells are covered by tree crowns and corresponds to a crown cover of 11%.

4 and 5, Landsat 7 and 8, covering a period of 32 years (Table 1). According to Gutman et al. (2008) these data have satisfactory radiometric and geometric qualities for performing land-use change analysis and in particular the historical analysis of deforestation. Due to a sensor failure (Scan Line Corrector or SLC) since 2003, the Landsat 7 images of the years 2005 to 2013 have high rates of missing data (leaf stripping) even if it has good geometric and radiometric qualities (Barsi et al., 2007). For each date, the six spectral bands B, G, R, NIR, SWIR1 and SWIR2 of the Landsat images of scenes p193r054 and p193r055 were mosaicked and projected to the coordinate reference system WGS 84 - UTM 31. All data manipulation and analysis of satellite images was done using the R environment for statistical computing (R Core Team, 2013) using the R-packages “raster” (Hijmans, 2019).

Classification of land covers change

Collection of tree cover training plots data

Accurate training plot data are essential for RandomForest classification. Several studies have shown that non-parametric machine learning algorithms, such as RandomForests, need a larger number of training data to attain optimal results (Potapov et al., 2012; Schneider, 2012). For obtaining a balanced set of training plots, the study followed a two-level sampling strategy. A random sample of 500 training plots was first selected and used them for the creation of an initial tree cover map. Based on this initial map a final sample of 5’402 training plots was drawn, stratified according to the tree cover observed in the initial map. The forest cover training plots were defined on the basis of the Landsat pixels (30 m × 30 m) and interpretation was done in QGIS based on high-resolution images of the year 2018 available in Google Earth (Quickbird). Based on a grid subdividing the training plots into nine cells, each training plot was assigned one of ten tree cover classes from 0 to 100% by counting the cells covered by tree crowns. These training plots served as the basis for the production of 2018 tree cover map. An example of visual interpretation of training plot is presented in Figure 2.

Classification with RandomForest

The RandomForest algorithm, developed by Breiman (2001), was selected for its good predictive capabilities for land-use classifications (Gislason et al., 2006) and time series analysis (Schneider, 2012). Several authors have shown that forest cover classifications with RandomForest outperform classifications with other types of algorithms such as maximum likelihood classification (Gislason et al., 2006; Schneider, 2012). RandomForest is a non-parametric supervised classification algorithm that combines the decision tree algorithm and an aggregation technique. The algorithm randomly selects a sample of observations and a sample of variables many times to produce a number of small classification trees (Breiman, 2001). “These small trees are then aggregated and a majority vote rule is applied to determine the final category” (Breiman, 2001). For this study the RandomForest implementation provided by the R-package "RandomForest" was used (Liaw and Wiener, 2002).

In order to improve the discrimination of different densities of tree cover, six indices derived from the spectral bands of the satellite images were calculated (1) the normalized vegetation index (NDVI) calculated as:

$$NDVI = (NIR-red)/(NIR+red) \quad (1)$$

where red and NIR stand for the spectral reflectance measurements acquired in the red (visible) and near-infrared regions, respectively (Rouse et al., 1974); (2) the enhanced vegetation index (EVI) is computed following this equation:

$$EVI = 2.5 \times (NIR-red)/(NIR+C1\times red - C2 \times blue + L) \text{ (Liu and Huete, 1995)} \quad (2)$$

where NIR/red/blue are atmospherically-corrected, L is the canopy background adjustment that addresses non-linear, differential NIR and red radiant transfer through a canopy, and C1, C2 are the coefficients of the aerosol resistance term, which uses the blue band to correct for aerosol influences in the red band. The coefficients adopted in Landsat are; L=1, C1 = 6, C2 = 7.5; (3) the Normalized Difference Moisture Index (NDMI) is calculated with the following equation:

$$NDMI=(NIR-MIR)/(NIR+MIR) \text{ (Jin and Sader, 2006)} \quad (3)$$

where MIR is the middle infrared; (4) the Soil Adjusted Vegetation Index (SAVI) is calculated as:

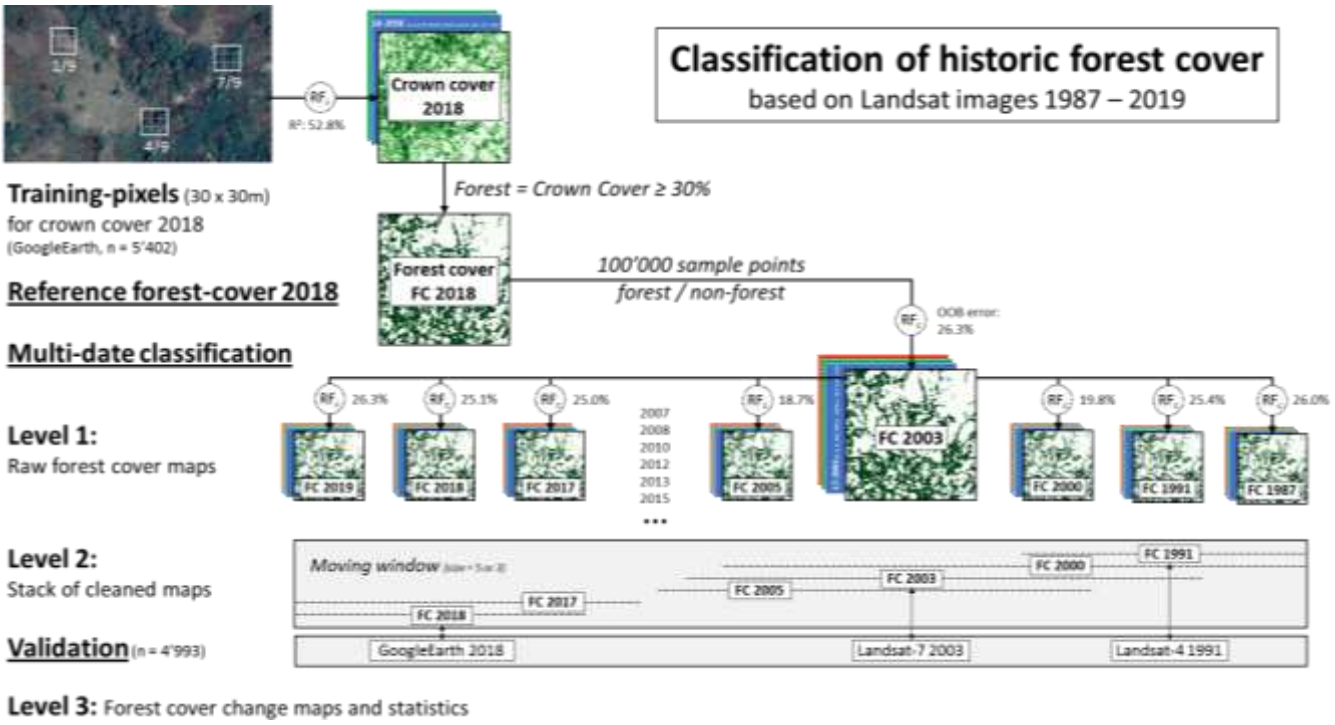

Figure 3. Flow chart of mapping of mapping deforestation from remote sensing and field forest inventory data: RF stand for Randomforest, FC for Forest cover, OOB stand for Out-of-bag.

Table 1. Acquisition date and sensor of Landsat images used for historical analysis of deforestation between 1987 and 2019. The covered WRS2 scenes are p193r054 and p193r055.

Year	Acquisition date	Sensor
2019	16/02/2019	L8 / OLI
2018	12/01/2018	L8 / OLI
2017	25/01/2017	L8 / OLI
2015	04/01/2015	L8 / OLI
2013	23/02/2013	L7 / ETM+ (SLC-off)
2012	04/01/2012	L7 / ETM+ (SLC-off)
2010	30/01/2010	L7 / ETM+ (SLC-off)
2009	27/01/2009	L7 / ETM+ (SLC-off)
2008	25/01/2008	L7 / ETM+ (SLC-off)
2007	22/01/2007	L7 / ETM+ (SLC-off)
2005	01/02/2005	L7 / ETM+ (SLC-off)
2003	27/01/2003	L7 / ETM+
2000	04/02/2000	L7 / ETM+
1991	10/01/1991	L4 / TM
1987	23/01/1987	L5 / TM

SAVI= (NIR-red) × (1+L)/(NIR+red+L) (Huete, 1988) (4)

where NIR is the reflectance value of the near infrared band, RED is reflectance of the red band, and L is the soil brightness correction factor; (5) the Modified Soil Adjusted Vegetation Index (MSAVI) is calculated as:

MSAVI= (NIR-red) × (1+L)/(NIR+red+L) (Qi et al., 1994) (5)

where RED is the red band reflectance from a sensor, NIR is the near infrared band reflectance, and L is the soil brightness correction factor. The difference between SAVI and MSAVI, however, comes in how L is calculated and (6) the Normalized Burn Ratio (NBR1 et NBR2) calculated as:

NBR = (NIR-SWIR)/(NIR+SWIR) (Key and Benson, 2005) (6)

where NIR is near-infrared and SWIR is short-wave infrared bands.

The utility of the different spectral bands and indices for the identification of classes: forest and non-forest has been tested with a recursive elimination of variables with the RFE algorithm available in the R-package "caret" (Kuhn, 2016). The most important variables for the prediction of tree cover were in the following order: SWIR2, SWIR1, NBR, NDMI and G but the best prediction of crown cover was obtained by using all six spectral bands and seven indices. 10-fold cross-validation, repeated three times, resulted with an R^2 of 52.9% and a mean error of the crown cover of 0.19.

Forest definition for the analysis of satellite imagery

The 7th Conference of the Parties of the United Nations Framework Convention on Climate Change (UNFCCC) adopted a general forest definition that allows some flexibility for national definitions: "Forest" is a minimum area of land of 0.05-1.0 hectares with tree crown cover (or equivalent stocking level) of more than 10-30 per cent with trees with the potential to reach a minimum height of 2-5 m at maturity in situ. A forest may consist either of closed forest formations where trees of various stories and undergrowth cover a high proportion of the ground or open forest. Young natural stands and all plantations which have yet to reach a crown density of 10-30% or tree height of 2-5 m are included under forest, as are areas normally forming part of the forest area which are temporarily un-stocked as a result of human intervention such as harvesting or natural causes but which are expected to revert to forest. The FAO definition of 'forest' includes all areas of at least 0.5 ha size with canopy cover of more than 10% of trees higher than 5 m, or trees able to reach these thresholds in situ (FAO, 2010). This is also the forest definition adopted by Togo. It may seem advantageous to define forest at this low canopy-cover threshold, because doing so would ensure that most lands that contain tree cover will be classified as forest and will thus be eligible for REDD+ incentives either through reduced degradation, reduced deforestation, or enhancement of carbon stocks. However, according to (Achard et al., 2014) these "thresholds cannot be 'measured' from Landsat satellite imagery with high accuracy" . A more "feasible assessment is that the canopy density be greater than 30%" (FAO and JRC, 2012). Most countries are defining forests with a minimum crown cover of 30% for UNFCCC reporting (FAO and JRC, 2012).

In case of this study forest was defined with a minimum canopy cover of 30% because the study area is the "forest zone" of Togo, where natural vegetation has canopy cover between 30 and 80% (Bastin et al., 2019) and lower rates are a sign of advanced forest degradation or beginning regeneration (fallows and secondary forests) within agricultural slash and burn cycles. Using this threshold, the tree cover map 2018 was converted to a corresponding forest cover map. Forest loss is used to refer to a scenario where a pixel loses forest cover and moves from above 30% crown cover threshold in a year, to below the threshold in a subsequent year. Forest gain was defined as the inverse of forest loss (Hansen et al., 2013).

Producing of forest cover maps

First the forest cover map 2018 was used for calibrating another reference map for the year 2003. Therefore, 100'000 pixels were randomly selected within a 3-pixel buffer around the forest edge 2018 and used the forest/non-forest observations in 2018 for classifying the 2003 image using again the RandomForest algorithm. By using this approach, the 2018 was reproduced using the satellite image 2003. The resulting forest cover map is as close as possible to the 2018 map. By using this approach of backward projection, it was implicitly assumed that a) the proportion of pixels that change land cover, i.e. the error introduced by using training pixels from another date is relatively small, b) the error is not biased (change from forest to non-forest at least partially compensated by changes from non-forest to forest) and c) the classification algorithm is relatively robust towards errors in the training data. There is a risk of methodologically induced bias if these conditions are not met. However, the criteria seem to be fulfilled by the study area and the classifier chosen. Nevertheless, 2003 the was used instead of the 2018 forest cover map as reference map for classifying all 15 Landsat images in the time-series using the same approach (Figure 3). Using the 2003 map in the middle of the analysed 32-year period (1987-2019) for calibrating further maps in both directions should reduce the risk of methodologically induced bias compared to using the 2018 map as reference for backwards projection only. Out of bag errors, a measure of disagreement of the resulting map with the classes of the 100'000 pixels used for calibration ranged between 19% and 26% depending on the number of years between the dates.

The raw forest/non-forest maps were cleaned by calculating for the 15 dates the majority class of each pixel, in a sliding window of size five. Thereby, a given pixel at a given date is assigned with the class that occurs most often in the pixel's series that includes the two precedent and following dates. For the second and the second last date in the series (1991 and 2018), a sliding window of size three was applied. Cleaning of the time series was repeated until convergence. Besides the smoothing of forest/non-forest transitions, this temporal filter also allows for filtering out noise from cloud and shadow and the missing values of the ETM+ SLC-off images. Forest cover changes were analyzed by comparison of the cleaned forest cover maps for the years 1991, 2003 and 2018. The initial and the last year of the series (1987 and 2019) were not considered in the analysis as they were not being cleaned at all because of missing anterior or posterior information and might thus contain a lot of noise compared to the cleaned images of the other dates.

Accuracy assessments of the estimates of forest cover changes

Assessing land cover change maps is known to be difficult and challenging (Hansen and Loveland, 2012) mainly due to "the difficulty in obtaining accurate land cover change reference datasets". Field surveys of historical change are constrained since "they involve questioning people with a deep knowledge of the area's history" (Grinand et al., 2013). Accurate assessment of forest cover change therefore requires particular attention. A total of 5'000 validation pixels (30m x 30m) were randomly selected from the study area and used for assessing the accuracy of the cleaned 1991, 2003 and 2018 forest cover maps and corresponding transitions. The forest/non-forest status of each validation pixel in the year 2018 was assessed by determining the tree cover within the pixel using high-resolution images for the year 2018 available in Google Earth (Quickbird) and considering as forest when tree cover is at least 30%. The forest/non-forest status for the years 2003 and 1991 was then determined by comparing Landsat images. If a change from forest to non-forest or vice versa could be observed compared to the 2018 image, their status was changed accordingly (Figure 4). For the resulting three-date transition classes the overall accuracy, Cohen's Kappa as well as the producer and user accuracy of the different classes were calculated including corresponding confidence intervals and area estimates as proposed by Olofsson et al. (2014).

Field validation of forest regeneration

The validation of the forest cover maps is complemented by a field mission for field control. Main objective was to get first-hand information

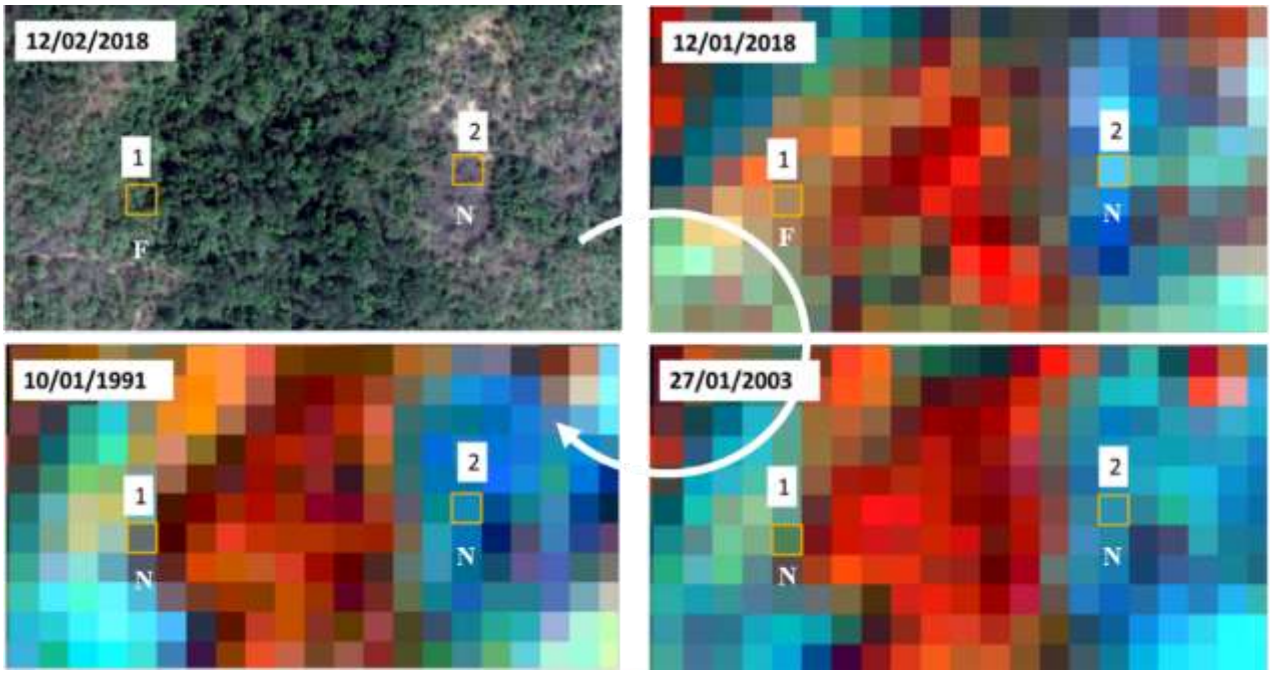

Figure 4. Examples of visual interpretation of validation plot for land cover change using QGis, QuickBird/Google Earth images and Landsat images. From top left to bottom right: cluster of training plots overlaying QuickBird images from Google Earth (12/02/2018) and Landsat (OLI, ETM+ and TM) false color composite RGB = 4, 5, and 3 acquired at dates 12/01/2018, 27/01/2003 and 10/01/1991.

information of the land-cover and land-use types where regeneration was detected on the maps. Therefore 106 pixels were randomly selected within the forest gain classes in the "Plaine of Litime" sub region and visited those locations in the field, determined current land-cover and land-use and assessed its history.

Validation with field data

The classification of satellite images was complemented by a field mission for field control. For this activity, geographical coordinates of the control points were acquired to ensure the accuracy of the classification carried out previously and in order to characterize the classification in the ground. To do this, a representative number (106 points) of field control points was selected in the change strata (forest gain) previously identified in the "plaine of Litime area". This method, based on the evaluation of control points, consists in verifying in the field the points previously identified during the classification for each of the land-use classes and in determining the percentage of verified points that actually correspond to those previously established.

Forest change rates estimation

The annual rate of forest change is calculated by comparing the area *A* under forest cover in the same region at two different times *t*. The standardized formula was used in the following equation proposed by (Puyravaud, 2003) for calculating the annual net forest cover change rates as well as rates of gross forest loss and regeneration.

Equation: $\theta = 1/(t2 - t1)\, ln\, A1/A2 \times 100$

RESULTS

Accuracy assessment of the model

Model accuracy assessment

The overall accuracy of the three-date transition map is 88.7% with Cohen's kappa of 82.4%. As shown in the error matrices (Table 3) producer and user accuracies were highest for non-change classes (90- 96%), medium for deforestation classes (62-94%) and lowest for regeneration classes (34-79%). Further, change detection looked to be more accurate for the 2003–2019 period (66- 96%) than for the 1991-2003 period (34-65%). Reasons might be lower radiometric quality of the satellite images, or lower quality of validation data used as reference due to the lack of high-res images for the first period.

Errors of commission and errors of omission are relatively well balanced for stable forest and non-forest classes. Forest loss and forest gain classes show a bit higher variation in the individual periods, but are also relatively well balanced over the whole period. When using these errors for adjusting mapped areas, slightly different figures than presented above were obtained, but figures that confirm the trends observed (Table 4).

In general, forest area is estimated to about 4.5% higher than those on the maps. However, the adjusted figures confirm the loss of about 15'000 ha forest cover in

Table 2. Accuracy assessment table according to Olofsson et al. (2014).

	Number of validation plot	FFF	FFN	FNF	FNN	NFF	NFN	NNF	NNN	U
FFF	1527	28.28	0.42	0.24	0.22	0.08	0	0.08	0.87	93.7 (±1.4)
FFN	301	0.68	4.62	0.23	0.34	0.04	0.15	0.06	0.23	72.8 (±4.0)
FNF	64	0.09	0	0.82	0.07	0.09	0	0.04	0.07	68.8 (±6.1)
FNN	167	0.09	0.19	0.36	1.97	0.15	0.09	0.09	0.21	62.3 (±6.6)
NFF	53	0.29	0	0.13	0.03	0.83	0	0.05	0.05	60.4 (±7.9)
NFN	27	0.02	0.09	0	0.02	0.05	0.33	0.02	0.09	51.9 (±14.7)
NNF	280	0.46	0.02	0.37	0.21	0.46	0.04	3.57	0.27	66.1 (±5.0)
NNN	2574	1.67	0.14	0.28	0.26	0.34	0.08	0.68	48.26	93.3 (±0.7)
P		89.5(± 1.2)	84.4(± 5.0)	33.8(±11.4)	63.1(±7.4)	40.6(±13.3)	47.5(±19.2)	77.6(±5.6)	96.4(± 1.0)	

Note: Proportional error matrix (% of mapped areas in a specific category), with User and Producer accuracy (in %). Overall accuracy is 88.7% with a 95% confidence interval of ± 0.8%.FFF: Forest 1991–2018; FFN, Forest loss between 2003 and 2018, FNN: forest loss between 1991 and 2003; NNN: No-forest; NNF: Forest gain between 2003 and 2018; NFF: Forest gain between 1991 and 2013.

first period. On the other hand they indicated that forest cover might even have increased in the second period. This second observation is however not significant, due to uncertainties in the adjusted forest areas (confidence interval of ±1.7%) (Table 5). The adjusted figures also confirm that gross deforestation nearly doubled from one period to the next where it compensated by increased regeneration.

Field validation

More than 80% of forest gains are low biomass formations such as fallows, forest recruits and in some cases oil palm plantations. Different types of forest formations are found in stable forest. These are dense forests, degraded dense forest, forested forest / savannah, agroforests, fallow, and sometimes plantations. These formations are called stable forest in the context of this study as long as they kept their state between 1991 and 2018.

Forest cover and forest cover change

The resulting maps show an overall decrease of the forest area during the last 30 years by about 6.7%, from 246’915 ha in 1991 to 230'390 ha in 2018 (Table 2). The corresponding forest cover in the study area thereby dropped from 40.9% to 38.1% (Figure 6). Net annual loss of forest cover was seven times higher in the period 1991-2003 (-0.49%) than in the period 2003-2018 (-0.07%). a different picture was seen when comparing gross forest loss. There, the rate increased from 0.94% in the 1991-2003 period to -1.33% in the 2003-2018 period (Figure 7). The forest regeneration compensated only half of the forest loss in the first period, or more or less completely compensated for deforestation observed in the second period. In the study area, forest area loss and forest regeneration was generally small-scale at the edge of forests. Variability of the annual de-forestation rate was observed, depending on the study area.

The forest loss rate (2.23% year^{-1}) occurred in the Kpele area (a part of the study area) is higher than the average forest loss rate in the study area in the period 1991 to 2018 (Figures 5 and 6). In the same period, the rate of forest loss in the “Plaine of litime” site is 0.068%·yr−1 (Figure 6). The low forest loss rate in “Plaine of litime” can be explained by the land use system in that area. Indeed, this area (cocoa plantation area) is characterized by different forest types that mix up with fallows, secondary forests and cocoa plantations (Soussou, 2009). The area is known for the systematic destruction of forests for growing of cocoa (Nyassogbo et al., 1996). There is not a clear boundary between forest and agriculture area in that region. This mix up is difficult to be detected as forest loss because the cocoa plantation and agroforest are forest according to the forest definition based on canopy cover solely. The high rate of deforestation in Kpele area can be explained by the conversion of forest mainly for shifting cultivation and palm oil

Table 3. Estimated areas of transition categories as obtained by the maps and the adjusted values incl. confidence intervals following the guidelines provided by Olofsson et al. (2014).

	Number of validation plot	Mapped area	Adjusted area (validation plots)	Confidence interval	
		ha	ha	ha	%
FFF	1527	182,257	190’745	± 3’715	1.9
FFN	301	38,372	33’097	± 2’462	7.4
FNF	64	7,195	14’650	± 2,235	15.3
FNN	167	19,089	18,847	± 2,273	12.1
NFF	53	8,309	12,367	± 2,104	17.0
NFN	27	3,801	4,153	± 1,239	29.8
NNF	280	32,628	27,793	± 2,488	9.0
NNN	2574	312,319	302,318	± 3,734	1.2

FNN: Forest loss between 1991 and 2003; NNN: No-forest; NNF: Forest gain between 2003 and 2018; NFF: Forest gain between 1991 and 2013.

Table 4. Estimated forest area in 1991, 2003 and 2018 according to Olofsson et al. (2014).

	Mapped area (ha)	Adjusted area (validation plots) (ha)	Confidence interval	
1991	246,915	256,854	± 4,045	1.6
2003	232,741	241,194	± 4,152	1.7
2018	230,390	245,364	± 4,286	1.7

Table 5. Evolution of forest and change area in 1991, 2003 and 2018.

Year	1991	2003	2018
Forest area (ha)	246,915	232,741	230,390
Period	1991-2003	2003 - 2018	1991-2018
Forest loss (ha/year)	-2,190 (-0.94%)	-2,812 (-1.33%)	
Forest gain (ha/year)	+1,009 (+0.40%)	+2,655 (+1.05%)	
Net change (ha/year)	-1,181 (-0.49%)	-157 (-0.07%)	
Net change (ha/year)	-	-	612 (-0.26%)

plantation (Table 6).

DISCUSSION

Forest cover dynamic

The results show, that forest cover in the area is highly dynamic. Gross forest loss and forest gain, to a large extent; compensate for each other and that net forest cover change is just a fraction of the overall dynamic observed. Together with the facts, that changes occur often gradual, disperse and on small scales, makes it extremely difficult to quantify net forest cover change. The comparison of independently produced forest/non-forest maps, might not be able to capture those dynamics accurately as minor deviances in the definition of the class “forest” leads to considerable differences between the maps that have nothing to do with changes on the ground and true changes might remain unobserved (Hansen and Loveland, 2012).

Direct, multi-date classification is often suggested as a more accurate method for mapping of lanes, avoiding to a certain extent the use of different “forest” definitions (GFOI, 2016). However, in such complex situations and with a lack of high-resolution historical imagery, it seems

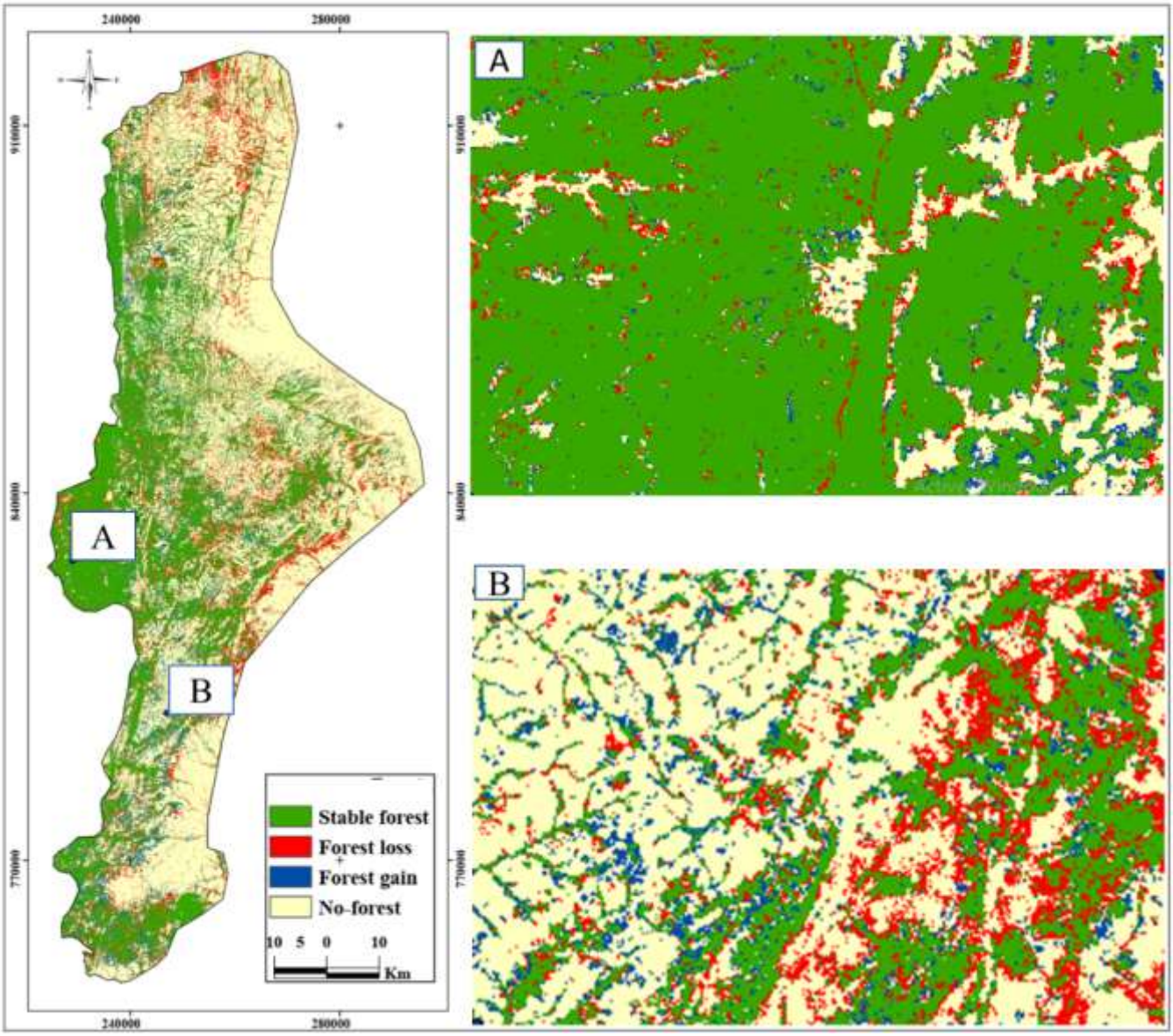

Figure 5. Forest cover change map for the period 1991 to 2003: A in kpele area; B in “plaine de Litime

to be far from evident to correctly attribute transition classes to training plots. Further, it is nearly impossible doing this just for a two-date comparison, but a whole time-series, with a sufficient number of training plots in order to ensure that all transition categories that are to be mapped are sufficiently represented.

The approach used in this study combines the above mentioned approaches and thereby overcomes many of those obstacles. A single date forest/non-forest map is produced based on available high-resolution images. For the classification of all other dates, the same forest definition is enforced by calibrating the classifier with this reference image. As a result, forest/non-forest maps that are most similar were obtained one to another; thus underestimating rather than overestimating land-cover changes.

Once the reference map is defined, this approach allows for automatic classification of time-series of several images. The advantage of time-series is that it can be used for cleaning the resulting maps. Time-series approaches have many other advantages, as they are not so dependent on the conditions at the time the individual images were collected (GFOI, 2016; Kennedy et al., 2007; Zhuravleva et al., 2013). In this study, a simple majority filter was used, but more complex rule-based filters for filtering out for example forest loss and regeneration in agricultural rotation cycles is possible. The longer the time-series at disposal, the better are the

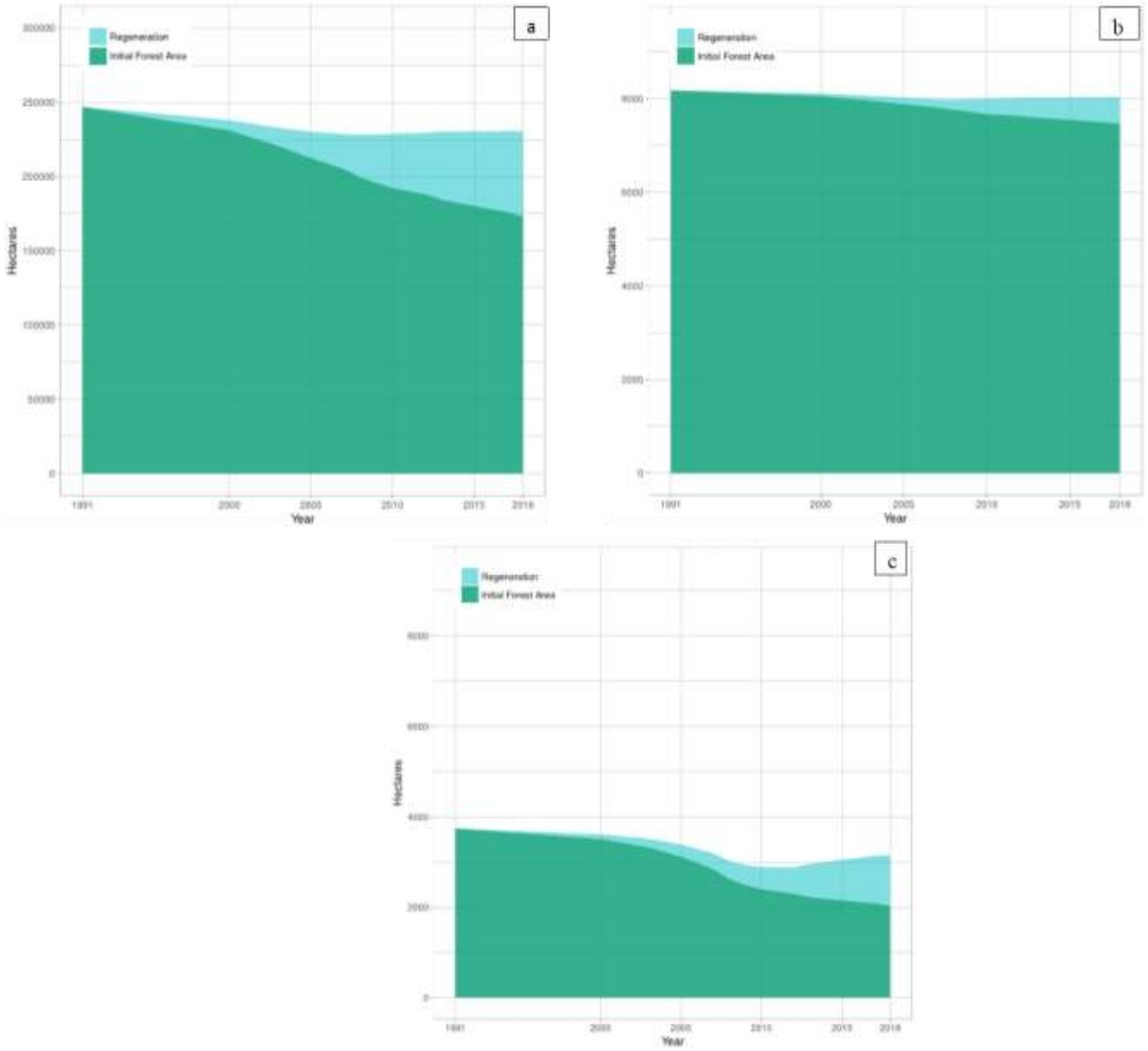

Figure 6. Evolution of forest area respectively in: a) the ecological zone VI, b a part of Kpele prefecture and in a portion of "Plaine of Litime.

possibilities for tracking land-use changes instead of just land-cover changes (Broich et al., 2011; GFOI, 2016).

The same approach could also be used for continuous monitoring, where time-series would be reevaluated annually with recently acquired Landsat images and with additional reference maps whenever new high-resolution data becomes available (Cohen et al., 2003). In principle it would even be possible to do the same analysis using a different forest definition (such as 10% crown cover) or doing analysis with different crown covers in order to assess forest degradation and regeneration within forests. Although there seems to be room for improvement, the study probably provides the most accurate figures on forest cover change available in Togo. The Cohen's kappa of the three-date forest/non-forest transition map (1991-2003-2018) is 82% which, according to Pontius (2000), shows that the map is accurate.

Various forest cover change estimation rates

This paper shows that for all study areas combined the net forest lost is 0.5% during the 1991-2003 period, 0.1% during 2003-2018 period, 0.2% during 2000-2015 period and 0.4% during the 1991-2000 period. There are very few studies on forest cover change in Togo based on

consistent methodology. Therefore, it is difficult to compare the results of this study with those of similar studies in the country since the methodologies and the forest definition are not the same. Nevertheless, the study investigated the results of this study by comparing them with previous studies in the country.

Togo is recognized to be part of countries with the highest annual deforestation rate (5.1%·year^{-1}) (FAO, 2010). Previous studies of forest cover had included the land use map using RapidEye satellite images 2013/2014; the interpretation of aerial photos taken between 1976 and 1985 and Landsat image from 1990 to 2015 (MERF 2018). The latter recorded a decrease of forest loss rate from 0.733 % in 1990-2000 period to 0.2% between 2000-2015. Forest loss rate was compared to the forest loss rate presented in this paper even if the area and the period are not the same. The same forest loss rate was found on the overlapping period (2000-2015).

Significant difference was found comparing (FAO, 2010) forest loss rate to the rate of deforestation of this study. Three possible explanations were identified for these marked differences. First, FAO rate of forest loss is based on estimation of national data. Secondly, the definition of forest was not exactly the same in the two studies (10% vs. 30 crow cover). Finally, the exact period and the details methodology of FAO estimation were not known.

According to Mayaux et al. (2013), net deforestation of African rainforest is estimated at 0.28% year^{-1} for the period 1990–2000 and 0.14% year^{-1} for the period 2000-2010. The forest loss rate in the study area (0.4% year^{-1}) for the period 2000-2010 is higher than the forest loss rate in West Africa in the same period. However, the forest loss rate in the study area (0.26% year^{-1}) for the period 1991 to 2018 is very close to forest loss rate in West area even if the period considered are not exactly the same.

Composite-based approaches have proved successful for large scale change mapping and been used for making global maps of tree cover change at annual basis (Hansen et al., 2013).

Remaining forests status

This study shows, that overall forest cover did not change significantly over the last decade and that forest loss was compensated by forest gain. However, this study does not provide an answer whether the quality of the forests lost and those gained are the same. Are the forests lost just fallows and secondary forest cleared in the agricultural cycle and continuously compensated with fallows on abandoned land elsewhere? Or to what extent does this forest loss concern dense or open forests that are newly converted to agricultural land and masked with increased abandonment of agricultural land?

Several previous studies (Adjossou, 2004, 2009; Adjossou and Kokou, 2004; Adjossou et al., 2019) have shown that the remaining forests in the sub-humid mountainous area today is very fragmented and is practically reduced to forest buffers in hard-to-reach areas and along rivers. Based on the field observation, the majority of remaining forest are agroforests, fallow and early secondary forest. These remaining forests are technically “forests” in the forest definition above. The agroforest which is an agricultural land is considered as forest according to the definition of forest in this study. The low rate of forest loss from this study can be explained by the fact that there is small-scale clearance at forest edges difficult to visual on Landsat image (Grinand et al., 2013). The small-scale clearance is mainly for shifting cultivation and logging. Therefore, open-canopy areas, secondary forest or plantations in the estimates of forest areas were included. The analysis is therefore limited to forest cover. Land use was not a consideration in the mapping as in the study of Hansen et al. (2013).

Further research is needed on this issue: assessing quality of forests (such as biomass), degradation and regeneration within forests (not just forest/non-forest), longer time-series and analysis of land-use patterns instead of land-cover solely.

Conclusion

This study has updated forest cover statistics and assessed the rate of forest change in the forest zone in Togo. Even if this rate of forest loss slowdown from 2003-2018, the status of the remaining forest (mainly fallow and degraded forest) should alert all stakeholders working to preserve the remaining forest in the forest zone of Togo. Coupled with rigorous work to delimit training and validation plots by photointerpretation, this study provides a method for monitoring the forest dynamics. This research responds to the necessity of capturing local forest change dynamics for small scale. However, the use of Landsat images may not be satisfactory given its relatively low spatial resolution to detect very small scale of forest cover change. Therefore, the availability of higher resolution images such as orthophoto, SPOT 6, Sentinel-2 or radar could be very beneficial in the analysis and validation of time-series of Landsat images. For example, the Sentinel-2 mission will generate data that when combined with Landsat data will enhance time series analysis of forest cover change. This research can support policy approaches towards reducing emissions from deforestation and degradation (REDD+) in Togo. Regular updates to these data are very important to enable more rapid and adaptive response to forest loss threats in Togo.

The information content of the presented datasets, provides a consistent basis on which to quantify critical

environmental issues, including (i) the drivers of the mapped forest cover change; (ii) the biomass mapping and associated emissions of disturbed forest areas; (iii) the status of remaining forests; (iv) the economic drivers of natural forest conversion to more intensive land uses; (vi) the relationships between forest dynamics and social welfare, health and (v) forest dynamics associated with governance and policy actions.

DATA AVAILABILITY

The data regarding this research work will be readily available when requested.

CONFLICT OF INTERESTS

The authors have not declared any conflict of interests.

REFERENCES

Achard F, Beuchle R, Mayaux P, Stibig HJ, Bodart C, Brink A, Carboni S, Desclée B, Donnay F, Eva H (2014). Determination of tropical deforestation rates and related carbon losses from 1990 to 2010. Global Change Biology 20(8):2540-2554. https://doi.org/10.1111/gcb.12605

Achard F, Eva H, Stibig HJ, Mayaux P, Gallego J, Richards T, Malingreau JP (2002). Determination of deforestation rates of the world's humid tropical forests. Science 297(5583):999-1002. https://doi.org/10.1126/science.1070656

Adjonou K, Bellefontaine R, Kokou K (2009). The open forests of the Oti-Kéran National Park in North Togo: Structure, dynamics and impacts of recent climate changes. Science et Changements Planétaires/Sécheresse 20(4):394-396. https://doi.org/10.1684/sec.2009.0211

Adjossou K (2004). Floristic diversity of forests bordering ecological zone IV of Togo. [DEA Thesis, Developmental Biology, Applied Plant Biology Option]. University of Lome.

Adjossou K (2009). Diversity, structure and dynamics of vegetation in the fragments of rainforests in Togo: The challenges for biodiversity conservation [Phd thesis]. University of Lome.

Adjossou K, Dangbo F, Houngbedji T, Abotsi K, Koda D, Guelly A, Kokou K (2019). Forest land use and native trees diversity conservation in Togolese mega hotspot, Upper Guinean, West *Africa*. https://doi.org/10.5897/jene2019.0799

Adjossou K, Kokou K (2004). Importance actuelle des forêts riveraines sur la conservation de la diversité biologique au Togo. In Biotechnologies Végétales, Biodiversité et Biosécurité: Défis et enjeux, Actes des IXèmes Journées Scientifiques Francophones ((Ed.). Presses Offset CTCE, p. pp 40-43). Dieudonné GOUMEDJOE.

Barsi J, Hook S, Schott J, Raqueno N, Markham B (2007). Landsat-5 thematic mapper thermal band calibration update. IEEE Geoscience and Remote Sensing Letters 4(4):552-555. https://doi.org/10.1109/lgrs.2007.896322

Bastin JF, Finegold Y, Garcia C, Mollicone D, Rezende M, Routh D, Zohner C, Crowther T (2019). The global tree restoration potential. Science *365*(6448):76-79. https://doi.org/10.1126/science.aax0848.

Breiman L (2001). Random forests. Machine Learning *45*(1):5-32.

Broich M, Hansen M, Potapov P, Adusei B, Lindquist E, Stehman SV (2011). Time-series analysis of multi-resolution optical imagery for quantifying forest cover loss in Sumatra and Kalimantan, Indonesia.

International Journal of Applied Earth Observation and Geoinformation 13(2):277-291. https://doi.org/10.1016/j.jag.2010.11.004

Cohen W, Maiersperger T, Gower S, Turner D (2003). An improved strategy for regression of biophysica l variables and Landsat ETM+ data. Remote Sensing of Environment 84(4):561-571. https://doi.org/10.1016/s0034-4257(02)00173-6

Ern H (1979). Die Vegetation Togos. Gliederung, Gefährdung, Erhaltung. Willdenowia 295-312.

FAO (2010). Global forest resources assessment. Main Report, FAO Forest Paper 163.

FAO JRC (2012). Global forest land-use change 1990-2005-Recherche Google. https://www.google.com/search?q=+Global+forest+land-use+change+1990%E2%80%932005&ie=utf-8&oe=utf-8&client=firefox-b-ab

Foley J, DeFries R, Asner G, Barford C, Bonan G, Carpenter S, Chapin F, Coe M, Daily G, Gibbs H (2005). Global consequences of land use. Science 309(5734):570-574. https://doi.org/10.1126/science.1111772

GFOI (2016). Méthodes et pratiques recommandées par l'Initiative mondiale pour l'observation des forêts-Recherche Google. https://www.reddcompass.org/download-the-mgd

Gislason P, Benediktsson J, Sveinsson J (2006). Random forests for land cover classification. Pattern Recognition Letters *27*(4):294-300. https://doi.org/10.1016/j.patrec.2005.08.011

Grinand C, Rakotomalala F, Gond V, Vaudry R, Bernoux M, Vieilledent G (2013). Estimating deforestation in tropical humid and dry forests in Madagascar from 2000 to 2010 using multi-date Landsat satellite images and the random forests classifier. Remote Sensing of Environment 139:68-80. https://doi.org/10.1016/j.rse.2013.07.008

Gutman G, Byrnes R, Masek J, Covington S, Justice C, Franks S, Headley R. (2008). Towards monitoring land-cover and land-use changes at a global scale: The Global Land Survey 2005. Photogrammetric Engineering and Remote Sensing 74(1):6-10.

Hall J, Swaine M (1976). Classification and ecology of closed-canopy forest in Ghana. The Journal of Ecology 913-951. https://doi.org/10.2307/2258816

Hansen M, Loveland T (2012). A review of large area monitoring of land cover change using Landsat data. Remote Sensing *of* Environment 122:66-74. https://doi.org/10.1016/j.rse.2011.08.024

Hansen M, Potapov P, Moore R, Hancher M, Turubanova S, Tyukavina A, Thau D, Stehman, S, Goetz S, Loveland T (2013). High-resolution global maps of 21st-century forest cover change. Science *342*(6160):850853. https://doi.org/10.1126/science.1244693

Hijmans R (2019). Introduction to the'raster'package (version 2.9-5).

Houghton R (2012). Carbon emissions and the drivers of deforestation and forest degradation in the tropics. Current Opinion in Environmental Sustainability 4(6):597-603. https://doi.org/10.1016/j.cosust.2012.06.006

Houghton R, Greenglass N, Baccini A, Cattaneo A, Goetz S, Kellndorfer J, Laporte N, Walker W (2010). The role of science in Reducing Emissions from Deforestation and Forest Degradation (REDD). Carbon Management 1(2):253-259.

Huete A (1988). A soil-adjusted vegetation index (SAVI). Remote Sensing of Environment *25*(3): 295-309. https://doi.org/10.1016/0034-4257(88)90106-x

Jin S, Sader S (2006). Effects of forest ownership and change on forest harvest rates, types and trends in northern Maine. Forest Ecology and Management *228*(1-3):177-186. https://doi.org/10.1016/j.foreco.2006.03.009

Kennedy R, Cohen W, Schroeder T (2007). Trajectory-based change detection for automated characterization of forest disturbance dynamics. Remote Sensing of Environment 110(3):370-386. https://doi.org/10.1016/j.rse.2007.03.010

Key C, Benson N (2005). Landscape assessment: Remote sensing of severity, the normalized burn ratio and ground measure of severity, the composite burn index. *FIREMON:* Fire Effects Monitoring and Inventory System Ogden, Utah: USDA Forest Service, Rocky Mountain Res. Station.

Kuhn M (2016). Contributions from Jed Wing, Steve Weston, Andre Williams, Chris Keefer, Allan Engelhardt, Tony Cooper, Zachary Mayer, Brenton Kenkel, the R Core Team, Michael Benesty, Reynald Lescarbeau, Andrew Ziem, Luca Scrucca, Yuan Tang, Can Candan and Tyler Hunt. Caret: Classification and regression training. R package version 6.0-73.

Liaw A, Wiener M (2002). Classification and regression by randomForest. R News 2(3):18-22.

Liu H, Huete A (1995). A feedback based modification of the NDVI to minimize canopy background and atmospheric noise. IEEE Transactions on Geoscience and Remote Sensing 33(2):457-465. https://doi.org/10.1109/36.377946

Liu J, Heiskanen J, Aynekulu E, Pellikka P (2015). Seasonal variation of land cover classification accuracy of Landsat 8 images in Burkina Faso. The International Archives of Photogrammetry, Remote Sensing and Spatial Information Sciences 40(7):455. https://doi.org/10.5194/isprsarchives-xl-7-w3-455-2015

Mayaux P, Pekel JF, Desclée B, Donnay F, Lupi A, Achard F, Clerici M, Bodart C, Brink A, Nasi R (2013). State and evolution of the African rainforests between 1990 and 2010. Philosophical Transactions of the Royal Society B: Biological Sciences 368(1625): 20120300. https://doi.org/10.1098/rstb.2012.0300

Ministère de l'Environnement et des Ressources Forestières (MERF) (2018). Traitement et analyse des données cartographiques issus des différentes études dans le cadre de la REDD+ p. 20. Coordination nationale REDD+.

Ministère de l'Environnement et des Ressources Forestières (MERF) (2013). Proposition de Mesures pour l'etat de preparation (R-PP) (p. 174). Fonds de partenariat pour le carbone forestier (FCPF), Ministère de l'Environnement et des Ressources Forestières.

Nyassogbo G, Gozo K, Ogounde L (1996). Economic crisis and socio-demographic changes in a plantation economy: The case of Litimé in Togo. Union pour l'étude de la population africaine.

Olofsson P, Foody G, Herold M, Stehman S, Woodcock C, Wulder M (2014). Good practices for estimating area and assessing accuracy of land change. Remote Sensing of Environment *148:*42-57. https://doi.org/10.1016/j.rse.2014.02.015

Pontius Jr (2000). Comparison of Categorical Maps. Photogrammetric Engineering & Remote Sensing 66(8):1011-1016.

Potapov P, Turubanova S, Hansen M, Adusei B, Broich M, Altstatt A, Mane L, Justice C (2012). Quantifying forest cover loss in Democratic Republic of the Congo, 2000-2010, with Landsat ETM+ data. Remote Sensing of Environment, *122:*106-116. https://doi.org/10.1016/j.rse.2011.08.027

Puyravaud JP (2003). Standardizing the calculation of the annual rate of deforestation. Forest Ecology and Management *177*(1-3):593-596. https://doi.org/10.1016/s0378-1127(02)00335-3

Qi J, Chehbouni A, Huete A, Kerr Y, Sorooshian S (1994). A modified soil adjusted vegetation index. Remote Sensing of Environment 48(2)119-126. https://doi.org/10.1016/0034-4257(94)90134-1

R Core Team (2013). *R:* A language and environment for statistical computing.

Rouse J, Haas R, Schell J, Deering D (1974). Monitoring vegetation systems in the Great Plains with ERTS.

Schneider A (2012). Monitoring land cover change in urban and peri-urban areas using dense time stacks of Landsat satellite data and a data mining approach. Remote Sensing of Environment 124:689-704. https://doi.org/10.1016/j.rse.2012.06.006

Soussou T (2009). Forest dynamics in the Litimé plain under anthropic pressure in Togo [PhD Thesis]. Aix-Marseille 3.

Tropek R, Sedláček O, Beck J, Keil P, Musilová Z, Šímová I, Storch D (2014). Comment on "High-resolution global maps of 21st-century forest cover change". Science 344(6187):981-981. https://doi.org/10.1126/science.1248753. https://doi.org/10.1126/science.1248753

UNFCCC (2010). Decision 1/CP.16, the Cancun Agreements: Outcome of the Work of the Ad Hoc Working Group on Long-Term Cooperative Action under the Convention. (UNFCCC Conference of the Parties). http://unfccc.int/2860.php

UNFCCC (2015). Draft Decision-/CP.20, Adoption of the Paris Agreement. (UNFCCC Conference of the Parties).

Zhuravleva I, Turubanova S, Potapov P, Hansen M, Tyukavina A, Minnemeyer S, Laporte N, Goetz S, Verbelen F, Thies C (2013). Satellite-based primary forest degradation assessment in the Democratic Republic of the Congo, 2000-2010. Environmental Research Letters *8*(2):024034. https://doi.org/10.1088/1748-9326/8/2/024034